Colloids and Surfaces B: Biointerfaces 254 (2025) 114787

Contents lists available at ScienceDirect

Colloids and Surfaces B: Biointerfaces

journal homepage: www.elsevier.com/locate/colsurfb

Mitochondrial activation via calcium peroxide/carrageenan/soybean lecithin-derived polypyrrole phototherapeutic microparticles

Sih-Chi Chuang [a,b,c,1], Shih-An Yu [c,1], Pei-Chia Hung [c,1], Andrew E.-Y. Chuang [d,e,f,1], Jia-Wei Liang [c,d,1], Chia-Lu Sun [g,1], Lekshmi Rethi [d,e], Hsu-Wei Fang [a], Hieu Trung Nguyen [h], Yao-Tung Tsai [i,j], Pei-Wei Weng [e,k,l,*]

[a] Department of Chemical Engineering and Biotechnology, National Taipei University of Technology, Taipei 10608, Taiwan
[b] Doctoral Program of Biochemical and Biomedical Engineering, National Taipei University of Technology, Taipei 10608, Taiwan
[c] Taipei Medical University Derived Company-Hsuan Chen Technology CO., LTD., New Taipei City 22055, Taiwan
[d] Graduate Institute of Biomedical Materials and Tissue Engineering, College of Biomedical Engineering, Taipei Medical University, New Taipei City, Taiwan
[e] International Ph.D. Program in Biomedical Engineering, College of Biomedical Engineering, Taipei Medical University, New Taipei City, Taiwan
[f] Cell Physiology and Molecular Image Research Center, Taipei Medical University-Wan Fang Hospital, Taipei 11696, Taiwan
[g] WELLCARE Health Care Supply Co., Ltd., Taipei, Taiwan
[h] Department of Orthopedics and Trauma, Faculty of Medicine, University of Medicine and Pharmacy at Ho Chi Minh city, Ho Chi Minh City 700000, Viet Nam
[i] Department of Orthopaedic Surgery, Tri-Service General Hospital, National Defense Medical Center, No. 325, Sec. 2, Chenggong Rd. Neihu Dist., Taipei City 11490, Taiwan
[j] Division of Traumatology, Department of Surgery, Tri-Service General Hospital, National Defense Medical Center, No. 325, Sec. 2, Chenggong Rd. Neihu Dist., Taipei City 11490, Taiwan
[k] Department of Orthopedics, School of Medicine, College of Medicine, Taipei Medical University, Taipei 11031, Taiwan
[l] Department of Orthopedics, Shuang Ho Hospital, Taipei Medical University, New Taipei City, Taiwan

ARTICLE INFO

Keywords:
Mitochondrial activation
Calcium peroxide
Carrageenan
Phototherapy
Polypyrrole microparticles

ABSTRACT

Mitochondria, often referred to as the "powerhouses" of eukaryotic cells, play a critical role in maintaining cellular homeostasis and supporting essential life functions, particularly in cell survival and apoptosis. This study introduces a composite formulation—combining carrageenan (Car), calcium peroxide (CaO_2), and microparticles, derived from soybean oil lecithin, enhanced with photothermally active polypyrrole (PPy)—to create Car-Lec-PPy MP, aimed at promoting mitochondrial activation in cells. The investigation focuses on intercellular mitochondrial transfer and activation as a therapeutic strategy. The formulation seeks to stimulate mitochondrial biogenesis and enhance cellular resilience through targeted mitochondrial activation, leveraging the synergistic effects of near-infrared (NIR) therapy. In the in vivo experiment, phototherapeutic Car-Lec-PPy MP was administered to rodent muscle tissue. The results showed increased expression of heat-shock proteins and reduced oxidative stress in the treated muscle. Preliminary findings suggest that this approach not only boosts mitochondrial activity but also improves cell proliferation and survival, presenting significant potential for applications in regenerative medicine and cellular therapy.

1. Introduction

Mitochondria [1–5] are often described as the powerhouses of eukaryotic cells due to their crucial role in maintaining cellular balance and essential functions, which are pivotal for both cell survival and death [6]. Research has increasingly linked a range of degenerative diseases, including pulmonary disorders, heart disease, and neurological damage, sarcopenia, to mitochondrial impairments [7–11]. To counteract this, there has been a growing interest in the innovative approach of managing impaired mitochondria with healthy ones in order to restore mitochondrial equilibrium. This method proposes a potential remedy for mitochondrial-related diseases [8,12]. Nonetheless, this approach is challenged by the need to preserve mitochondrial integrity during isolation and to manage the mitochondria's vulnerability outside

* Corresponding author.
E-mail address: wengpw@tmu.edu.tw (P.-W. Weng).
[1] These authors contributed equally.

https://doi.org/10.1016/j.colsurfb.2025.114787
Received 3 October 2024; Received in revised form 28 April 2025; Accepted 9 May 2025
Available online 12 May 2025
0927-7765/© 2025 Elsevier B.V. All rights are reserved, including those for text and data mining, AI training, and similar technologies.

the cellular environment post-isolation [13,14].

As an alternative, the method of intercellular mitochondrial activation or management has emerged as a promising solution, attracting significant scientific interest [14]. Recent investigations have highlighted this natural ability of cells, where mitochondria are actively transported from healthy to damaged cells in response to disease-induced stress [8,9,15]. However, the efficiency of this management is not yet adequate to fully reverse mitochondrial dysfunction due to the high demands of such processes [16,17]. Furthermore, the treating of mitochondria to affected cells presents a significant challenge, complicating the therapeutic use of this strategy due to potential safety concerns. As such, developing a rapid and precise method for the intercellular activation of mitochondria in cells is highly sought after. Such advancements are expected to lead to a significant reduction in cellular apoptosis, enhancement of cell survival, and restoration of cellular functions [18]. This perspective underscores the urgent need for improved technologies and methods that can safely and efficiently facilitate mitochondrial activation to re-establish cellular health and stave off disease progression. In this regard, enhancing the mitochondrial activities in cells has become an intriguing niche in cellular biology and regenerative medicine, mainly due to the pivotal role of cells in tissue repair and regeneration [19].

Previous research indicates that mild hyperthermia conserves mitochondrial functionality while diminishing the production of mitochondrial reactive oxygen species (ROS) [20]. Mitochondria are essential organelles encased within membranes, pivotal for maintaining cellular energy balance and metabolic processes, as well as in facilitating signaling and apoptosis. Aryl hydrocarbon receptors (AhRs), which are ligand-activated transcription factors, play a significant role in recognizing and responding to a broad spectrum of xenobiotics, including polyaromatic hydrocarbons and dioxins, by initiating various detoxification pathways. These receptors are also activated by natural dietary substances and endogenous metabolites. Moreover, AhRs influence the regulation of a wide range of genes that are crucial for mitochondrial biogenesis and function. According to prior studies, certain aromatic hydrocarbon compounds, when interacting with AhRs and administered in low doses, exhibit a hormesis-like effect that is particularly beneficial for mitochondrial function, a phenomenon known as mitohormesis [21].

The relationship between AhRs and mitochondria underscores a complex interplay where environmental and dietary factors can modify mitochondrial dynamics. This interaction not only helps the cell adapt to environmental toxins but also enhances its metabolic efficiency and stress response capabilities. The process of mitohormesis, wherein low-level exposure to certain stressors induces a beneficial adaptive response in mitochondria, is gaining attention for its potential therapeutic implications in aging and disease prevention. Understanding how AhRs modulate mitochondrial responses can pave the way for innovative approaches to manage mitochondrial diseases, improve cellular resilience, and optimize metabolic health through dietary and environmental interventions.

According to the literature, various biomedical materials, including polysaccharides and conducting polymers have shown positive effects on mitochondrial activation [22]. In this study, we hypothesize and propose an approach utilizing carrageenan (Car) encapsulating calcium peroxide (CaO_2) polymerized phototherapeutic polypyrrole (PPy) preserving aromatic hydrocarbon-like compounds as well as soybean oil (Lecithin)-based microparticle (Car-Lec-PPy MP) formulation for enhancing mitochondrial activation, as indicated in Scheme 1. This composite Car-Lec-PPy MP holds promise as a biologically tolerated material for cell engineering and regenerative medicine applications [23,24]. Recent observations have revealed the unique biological effects of this composite microformulation in regulating the expression of key functional biomarkers in cells and muscle tissues, including Aryl hydrocarbon Receptor (AhR), Rhodamine 123 (RH123), Heat Shock Proteins (HSP), Rhodamine 123, 5-Ethynyl-2 ´-deoxyuridine (EDU), and Amplex Red. These biomarkers are critical for facilitating intercellular mitochondrial activation, influencing processes such as cellular respiration, stress response, and cell proliferation.

Given the essential roles these biomarkers play in mitochondrial dynamics, the development of photothermally active Car-Lec-PPy MP-based technology offers a promising approach to enhance mitochondrial transfer rates within cells and tissues. This strategy not only supports more efficient mitochondrial replenishment but also addresses the broader challenge of cellular energy deficits and oxidative stress, potentially improving outcomes in regenerative medicine and cellular therapies. By leveraging the synergistic effects of NIR phototherapy, this

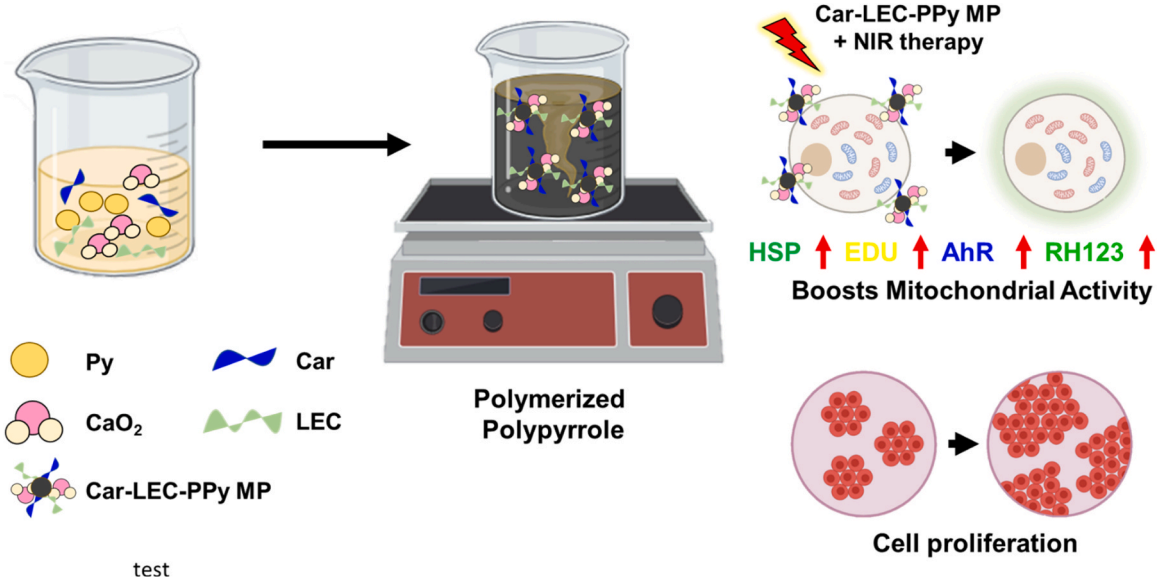

Scheme 1. Schematic representation of the proposed Car-Lec-PPy MP formulation for enhancing mitochondrial activation. The formulation consists of carrageenan (Car) encapsulating calcium peroxide (CaO_2), polymerized with photothermally active polypyrrole (PPy), and combined with soybean oil-derived lecithin-based microparticles. The composite microparticles facilitate mitochondrial activation through targeted delivery and near-infrared (NIR) phototherapy. This mechanism enhances mitochondrial biogenesis, cellular resilience, and functional biomarker expression in cells and tissues, promoting improved cell proliferation and stress response. The image was edited by BioRender.

composite formulation provides a targeted, non-invasive method to stimulate mitochondrial biogenesis and activity. These capabilities make it a powerful tool for applications ranging from muscle repair and tissue regeneration to broader therapies aimed at combating age-related mitochondrial decline and metabolic disorders.

2. Experimental section

2.1. Materials

The pyrrole monomer (Py), carrageenan (Car), calcium peroxide (CaO_2), 4′,6-diamidino-2-phenylindole (DAPI), fluorescein isothiocyanate (FITC), DAPI, and Propidium Iodide (PI) were acquired from Sigma–Aldrich (St. Louis, Missouri, USA). The L929 line of fibroblasts was sourced from the American Type Culture Collection (ATCC, Manassas, 10801 University Blvd, USA). Additionally, the cell viability assay kit, specifically the Live/Dead kit, was procured from Thermo Fisher Scientific (Waltham, MA, USA). The AhR, HSP and RH123 antibodies conjugating fluorescent dyes, Rhodamine 123, EDU, and Amplex Red were obtained from Abscience Co., Ltd. (Taipei City, Taiwan). Lecithin (LEC, soybean-based concentrate) was obtained from Bao Geng Biotechnology Co. (New Taipei City, Taiwan), Dulbecco's Modified Eagle Medium (Gibco DMEM, Thermo Fisher, Waltham, MA USA), Fetal Bovine Serum (Bioidea, Tehran, Iran) and streptomycin/penicillin (Gibco, Thermo Fisher, Waltham, MA USA), 3-(4,5-dimethylthiazol-2-yl)-2,5-diphenyl tetrazolium bromide (MTT, Invitrogen, Thermo Fisher Scientific, Waltham, MA USA), Phosphate Buffer Saline(PBS, Gibco, Thermo Fisher, Waltham, MA USA), dimethyl sulfoxide (DMSO, Merck, Neihu District. Taipei, Taiwan), paraformaldehyde solution (Sigma-Aldrich, St. Louis, Missouri, USA), Triton X-100 (Merck, Neihu District. Taipei, Taiwan)

2.2. Preparation and characterizations of the Car-Lec-PPy MP

In order to ascertain the optimal formulation (Car-Lec-PPy MP), we analyzed different mass ratios of the constituent materials LEC, Car, CaO_2, and Py. The ratios were 170/10/20/20, 170/10/20/50, 170/10/20/80, 170/10/20/110, and 170/10/20/140(mg/mL). The materials underwent mixing using a magnetic stirrer (100 revolutions per minute (rpm)) at the ambient temperature. Afterwards, we carefully assessed the development of the resulting particles. The analysis employed Dynamic Light Scattering (DLS,Malvern Panalytical, Malvern, United Kingdom) to measure the particle size, Polydispersity Index (PDI), and zeta potential of the particles formed. The size and zeta potential were also checked with PBS and PBS+ 10 % BSA to ensure the properties at different time periods. Elemental analysis of Car-Lec-PPy and Car-Lec-PPy +NIR was analyzed using SEM-EDAX for the Car-Lec-PPy, and Car-Lec-PPy +NIR groups, detecting changes in carbon, oxygen, calcium, sulfur, iron, and nitrogen levels post-NIR exposure.

In order to examine the changes in the structure of different formulations, the fluorescent FITC was added to the aqueous solutions at a concentration of 1 mg/mL during their development. This enables clear visualization of the formulation's structures under a fluorescence microscope, highlighting any morphological changes that occur during the experiment. In addition, the oxidation-reduction potential (ORP) of each sample was evaluated quantitatively to evaluate their oxidative or reductive states. A spectrometric meter was used to assess the polymerization level in the formulations. In addition, Fourier Transform Infrared Spectroscopy (FTIR, Nicolet iS 10, Thermo Scientific, Waltham, MA, USA) and a thermometer were used to examine the chemical characteristics and photothermal impacts of the formulations, respectively. This evaluation methodology is specifically developed to offer an in-depth comprehension of the physical, chemical, and thermal characteristics of the formulations being examined.

2.3. In vitro assessments

The viability and mitochondrial activation extent of the cells in contact with different compositions of formed materials was assessed using a Live/Dead assay that relies on the Calcein AM/ethidium homodimer-1 (EthD-1) kit. As per the instructions provided by the manufacturer, a volume of 100 μl of the Calcein AM/EthD-III solution was added to the samples containing cells on days 1 and 5 of the culture. The specimens were subjected to incubation at a temperature of 37 °C for a duration of 20 min, following which they underwent a thorough rinsing process using PBS. The materials were photographed using an inverted fluorescent microscope (Nikon TE 2000-U, Japan). The quantity of living (green) and apoptotic (red) cells was measured using ImageJ software. Cell viability was determined by calculating the ratio of live cells to the total number of cells in each sample set. This methodology enables a thorough examination of the biological compatibility and safety of formulations, which is essential for their prospective utilization in medical and tissue engineering domains. Utilizing Live/Dead assays offers a thorough assessment of the cytocompatibility of the samples being examined.

An analysis was conducted on the effects of the freshly produced formulations on the aryl hydrocarbon receptor (AhR) and RH123 (which indicates mitochondrial membrane potential) in L929 fibroblasts. Subsequently, the specimens were rinsed with PBS in order to remove any unbound compounds. Afterwards, the nuclei were stained by administering a DAPI or PI solution to the samples for a duration of 5 min. Following the completion of the staining procedure, the samples were observed and recorded using a fluorescent microscope. This technology enables accurate observation of the cellular and subcellular effects of the formulations. It can acquire insights on cellular arrangements, nuclear integrity, and cell viability by employing specialized stains such as rhodamine phalloidin, DAPI, and PI, respectively. Fluorescent microscopy is utilized in this context to not only verify the position and function of the AhR within the cell, but also to evaluate the general well-being of the mitochondria, as indicated by the membrane potential. A thorough examination of cells is essential for comprehending the biological interactions and possible therapeutic advantages of the formulations under investigation. To evaluate time-dependent cellular uptake, cells were incubated with FITC-labeled Car-Lec-PPy for different time points (0 min to 120 min). The fluorescence microscope was used to visualize particle internalization.

2.4. In vivo examinations

The animal operative and experimental procedures were approved by the Institutional Animal Care and Use Committee (IACUC, LAC No: SHLAC2024–0090 and SHLAC2024–0101) of Taipei Medical University. Male ICR mice (6–8 weeks old), weighing between 25 and 30 g, were obtained from BioLASCO (Taipei, Taiwan). A total of 24 ICR mice were used in this study. The mice were randomly divided into four experimental groups, with 6 animals per group. The groups included untreated control animals, animals subjected to near-infrared (NIR) exposure on their legs, animals receiving an intramuscular (IM) injection of Car-Lec-PPy MP in their legs, and animals treated with both the IM injection of Car-Lec-PPy MP and NIR exposure on their legs [25].

Post-treatment, the leg muscle, heart, liver, spleen, lung, and kidney tissues were harvested for further analysis. Tissues were fixed in 10 % formalin and embedded in paraffin. Tissue sections were cut into 4-μm slices and stained with hematoxylin and eosin (H&E). For immunohistochemistry, tissue slides underwent deparaffinization followed by epitope retrieval. The sections were then incubated with primary antibodies against AhR, HSP, and RH123 to assess immunoreactivity. Additionally, Rhodamine 123, EDU, and Amplex Red assays were performed to evaluate the biological responses of the tissues. Histological images were captured using optical microscopy, and fluorescence intensities were quantified with ImageJ software. Apoptosis was assessed

by DeadEnd™ Fluorometric TUNEL System (Promega, Madison, Wisconsin, USA), measuring DNA fragmentation via green fluorescence intensity in the Normal, NIR, Car-LEC-PPy, and Car-LEC-PPy+NIR groups.

The blood analyses were performed using automated analyzers with mouse-specific algorithms and parameters (IDEXX ProCyte Dx and Abaxis VetScan5). Red blood cells (RBC), white blood cells (WBC), reticulocytes, platelets, and schistocytes were quantified from whole blood collected via retro-orbital bleeding under anesthesia on day 14 post-treatment. Data comparisons between the Normall and Car-LEC-PPy+NIR were performed.

2.5. Statistical analysis

The statistical difference was analyzed by the One-Way ANOVA. The difference of $P < 0.05$ is considered statistically significant. Statistically significant differences were considered for $^{*}p \leq 0.05$, $^{**}p \leq 0.01$, $^{***}p \leq 0.001$ and $^{****}p \leq 0.0001$.

3. Results and discussion

3.1. Characterization of Car-LEC-PPy MP

For the formulation testing (Fig. 1), the mass ratios (LEC/Car/CaO_2/Py) were established at 170/10/20/20, 170/10/20/50, 170/10/20/80, 170/10/20/110, and 170/10/20/140 (mg/mL). An observed trend showed that increasing the Py content from 20 mg to 80 mg resulted in a reduction in particle size from approximately 9725 nm to 4821 nm. Conversely, increasing Py from 80 to 140 mg led to an increase in particle size from approximately 4821 nm to 9050 nm. This pattern suggests that the optimal polymerization of Py occurs at 80 mg, where it effectively integrates into the resultant Car-LEC-PPy microparticle (Car-LEC-PPy MP).

In this system, the polymerization of Py might be influenced by oxygen-dependent chemicals such as LEC and CaO_2, leading to the formation of a LEC-PPy complex. This complex is then encapsulated within the Car polymer to create a core-shell structure. According to the Dynamic Light Scattering (DLS) data (Fig. 1a), starting with a ratio of 170/10/20/20, approximately 9725 nm in size, was observed possibly due to

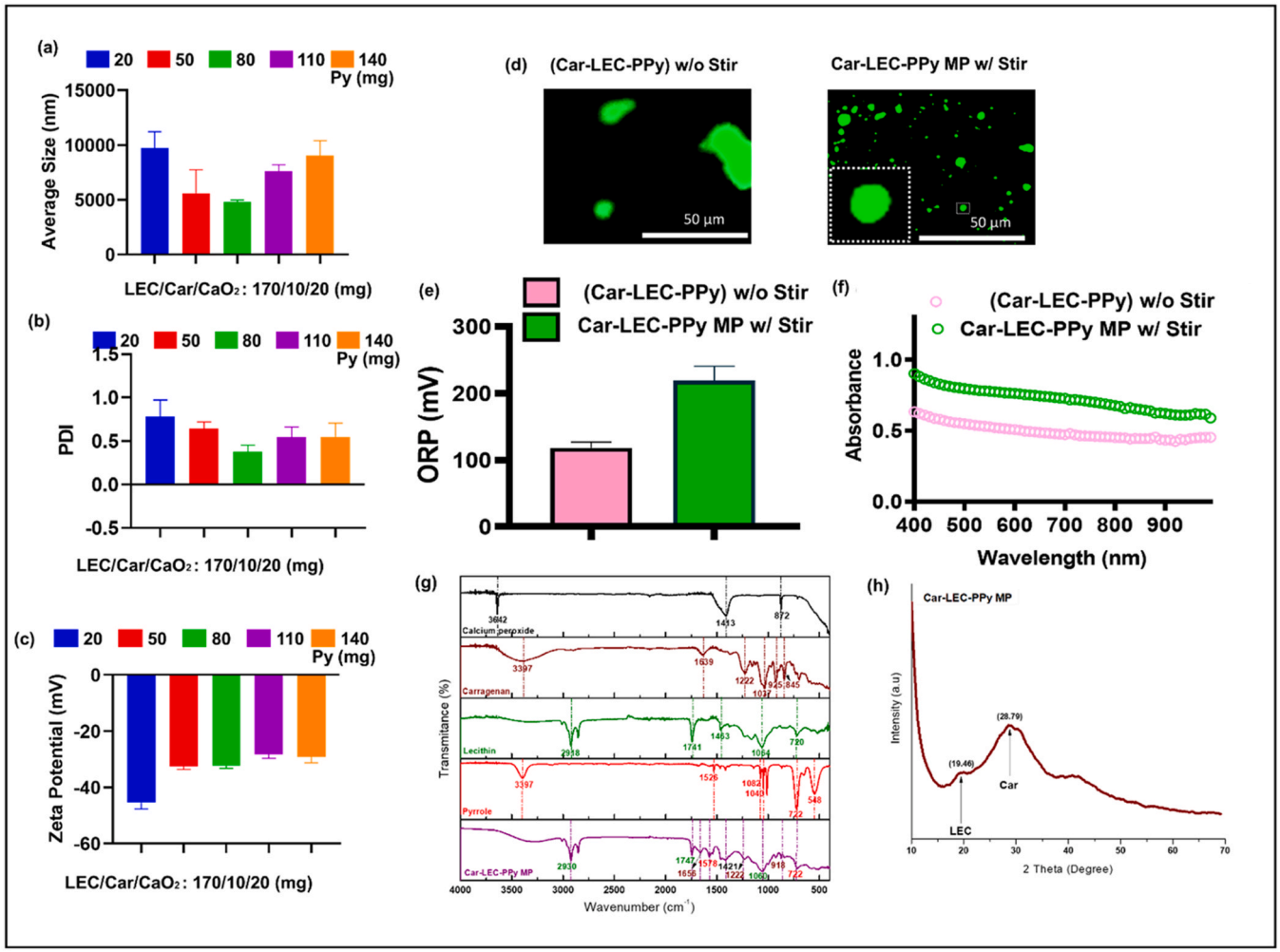

Fig. 1. Characterization of Car-LEC-PPy MPs. (a) Particle Size Distribution shows a decrease in size from ~10,000 nm to 5000 nm as Pyrrole (Py) concentration increases from 20 mg to 140 mg, then rises to ~9000 nm at 140 mg. (b) PDI Zeta Analysis identifies the optimal formulation (170/10/20/80) with a PDI below 0.5, indicating good uniformity and stability. (c) Zeta Potential of the optimal formulation is approximately −30 mV, highlighting the Car polymer's influence. (d) Fluorescence Microscopy reveals uniform particle distribution in stirred samples, while non-stirred samples show aggregation. The scale bar is 50 μm. (e) ORP Measurements show higher oxidation in stirred samples (200 mV) compared to non-stirred (100 mV). (f) Spectrometric Absorbance demonstrates greater absorbance and effective polypyrrole formation in stirred samples, suggesting NIR-photothermal potential. (g) FTIR of the composite's chemical composition. (h) XRD reveals crystalline phases at 19° and 28° within an amorphous structure. (i) Photothermal Response graph and thermal camera image display a rapid temperature rise to 47.8 °C under light, confirming effective photothermal conversion. These analyses highlight the composite's structure and potential applications.

intensified interactions during polymerization. Conversely, the ratio 170/10/20/50 yielded smaller particles, around 5611 nm, indicating enhanced crosslinking efficiency with increased Py concentration. Subsequent reductions in Py content for the ratios 170/10/20/80 and 170/10/20/110 resulted in a further change in average size to about 4821 nm and 7608 nm, respectively, reflecting a complex interplay of component concentrations on particle morphology. Lastly, despite higher Py content, the ratio 170/10/20/140 yielded a slightly reduced average size of about 9050 nm, highlighting non-linear relationships between Py concentration and particle size. The smallest particle size was achieved with the ratio LEC/Car/CaO_2/Py of 170/10/20/80, and this formulation was selected for further experiments.

The polydispersity index (PDI) data (Fig. 1b) shows that the Car-LEC-PPy MP maintained acceptable polydispersity. For the ratio 170/10/20/20, the PDI was approximately 0.8. As the Py content increased in subsequent ratios, namely 170/10/20/50, 170/10/20/80, and 170/10/20/110, the PDI values changed to approximately 0.7, 0.4, and 0.6, respectively. Interestingly, despite a higher Py content in the ratio 170/10/20/140, the PDI remained consistent at approximately 0.6. These findings suggest that variations in Py concentration influenced the particle size distribution within the formulations. Lower PDI values indicate a narrower particle size distribution, implying greater uniformity in particle sizes. Additionally, the zeta data (Fig. 1c) indicated that the Car-LEC-PPy MP was negatively charged, approximately −32 mV, likely due to the Car acting as a shell component.

As per previously published literature, in this polymerization monomers including thiophene, benzene, aniline, and pyrrole undergo chemical oxidative polymerization by various oxidizing agents [26]. CaO_2 is considered an oxidizing agent [27]. It serves as a source of hydrogen peroxide when it reacts with water, releasing oxygen in the process. This reaction makes CaO_2 useful in various applications that require the gradual release of oxygen over time, such as in environmental remediation for aerobic biodegradation of pollutants, in agriculture to oxygenate soil, and in the medical field for wound healing as an oxygen supplier. Its oxidizing properties are also utilized in formulations where a controlled oxidative environment is necessary, such as in certain polymerization processes. Further examination reveals that Car, the chosen anionic polymer for the Car component, is significant due to its anionic polysaccharide nature [28]. In addition, the utilization of κ-Carr alone has garnered interest due to its several prospective medicinal applications, including as its ability to operate as an anti-coagulant, anti-cancer, anti-hyperlipidemic, and immuno-modulatory agent [29].

Fluorescence microscopy data (Fig. 1d) revealed that the formulation consisting of LEC/Car/CaO_2/Py at a ratio of 170/10/20/80 mg, when subjected to magnetic stirring, produced uniformly distributed microparticles with excellent colloidal stability. The Car-LEC-PPy MP composite was analyzed both with and without stirring to evaluate the effects of the preparation method on particle. Conversely, the same formulation, when not subjected to magnetic stirring, showed a tendency for the particles to aggregate and precipitate, as evidenced by the fluorescence microscopy observations (Fig. 1d). The magnetic stirring likely imparts necessary shear forces that facilitate a microemulsion process, contributing to the uniformity of the Car-LEC-PPy microparticles distribution and electrochemical properties. The Car-LEC-PPy MP composite prepared without stirring exhibited larger particle sizes, while the composite prepared with stirring showed more homogeneously distributed particles. This homogeneity is clearly demonstrated by the green fluorescent labeling, which highlights the uniform dispersion of particles in the stirred sample.

Regarding the oxidation-reduction potential (ORP), data depicted in Fig. 1e indicates that the formula with magnetic stirring attained a higher ORP level (above 200 mV), compared to its counterpart without stirring, which maintained a lower ORP level (approximately 110 mV). This difference suggests that magnetic stirring enhances the contact area and interaction among components, allowing for a more complete chemical reaction. This reaction likely involves the oxidative effects from CaO_2 and LEC in the polymerization of Py, leading to increased oxidation levels as previously documented in chemical oxidative polymerization studies [30].

Spectrometric analysis (Fig. 1f) further corroborates these observations. The UV-Vis absorbance spectra of the non-stirred and stirred Car-LEC-PPy MP composites were measured across the wavelength range of 400–900 nm. The non-stirred mixture exhibited relatively lower absorbance throughout this range, indicating a less effective formation of the composite material. In contrast, the stirred formulation (Car-LEC-PPy MPs) demonstrated significantly higher absorbance across the same wavelength range. This increased absorbance is indicative of a more successful formation of polypyrrole, especially in its oxidized state. The presence of polypyrrole in its oxidized form is crucial as it directly contributes to the composite's enhanced spectral properties.

FTIR analysis was performed to confirm the structural characteristics and integration of the components in the Car-LEC-PPy MP composite (Fig. 1g). Calcium peroxide showed peaks at 3642 cm^{-1} (O-H stretching) and 872 cm^{-1} (O–O bridge). Carrageenan exhibited key bands at 3397 cm^{-1} (O-H), 1222 cm^{-1} (S-O), 1037 cm^{-1} (C-O-C), 925 cm^{-1} (C-O-SO_3), and 845 cm^{-1} (sulfate). Lecithin displayed peaks at 2918 cm^{-1} (C-H), 1741 cm^{-1} (C═O), 1463 cm^{-1} (CH_2 asymmetric stretching), 1229 cm^{-1} (C-O), and 1064 cm^{-1} (C-C). Pyrrole had characteristic peaks at 3397 cm^{-1} (N-H), 1526 cm^{-1} (C═C), 1082 cm^{-1} (C-N), and 722 cm^{-1} (C-H). The final composite exhibited distinct peaks that confirm the successful integration of the components into the composite [31–36].

XRD analysis of the Car-LEC-PPy MP composite showed peaks at 19° and 28°, indicating some crystalline regions within a mostly amorphous structure. The 19° peak may be due to the polymer matrix or interactions between lecithin and pyrrole, while the 28° peak could result from calcium peroxide or crystalline carrageenan. The broad XRD pattern suggests a high degree of molecular disorder, typical of complex polymeric materials. This mix of crystalline and amorphous regions contributes to the composite's unique properties, making it suitable for its intended applications (Fig. 1h) [37–39].

Additional analysis was done for the photothermal effect, stability, and morphological-elemental analysis (Fig. S1–3)

3.2. *In vitro assessments of Car-LEC-PPy MP*

The fluorescence microscopy data (Fig. S4) demonstrated that the FITC-labeled Car-LEC-PPy MPs were progressively taken up by L929 cells over time (0–120 min). The Live/Dead assay results further elucidate the biocompatibility and therapeutic potential of the Car-LEC-PPy MP in Fig. 2a. In the control group, which received no treatment, there were no dead cells observed, indicating the baseline health of the cell culture. Similarly, cells exposed to NIR light alone also showed fewer dead cells, confirming that NIR exposure by itself does not induce cytotoxicity. For the group treated with the Car-LEC-PPy MP composite and exposed to NIR light, minimal dead cells were observed, demonstrating that the composite, in conjunction with NIR exposure, does not harm the cells.

According to the data obtained through fluorescence microscopy (Fig. 2b), negligible expression of Aryl Hydrocarbon Receptor (AhR) was observed in both the control group of L929 cells and those exposed to NIR alone. In contrast, cells treated with Car-LEC-PPy microparticles, with or without additional NIR exposure, demonstrated significant AhR expression. This aligns with previous research indicating that AhR activation is a crucial process in the biological response to polycyclic aromatic hydrocarbons (PAHs) [40].

Further microscopic analysis presented in Fig. 2c revealed minimal expression of Rhodamine 123 (RH123) in the control and NIR-only groups. However, cells that were treated with Car-LEC-PPy MPs displayed noticeable RH123 expression, indicating changes in mitochondrial activity. RH123 is a fluorescent dye known for its selective accumulation in mitochondria based on their membrane potential,

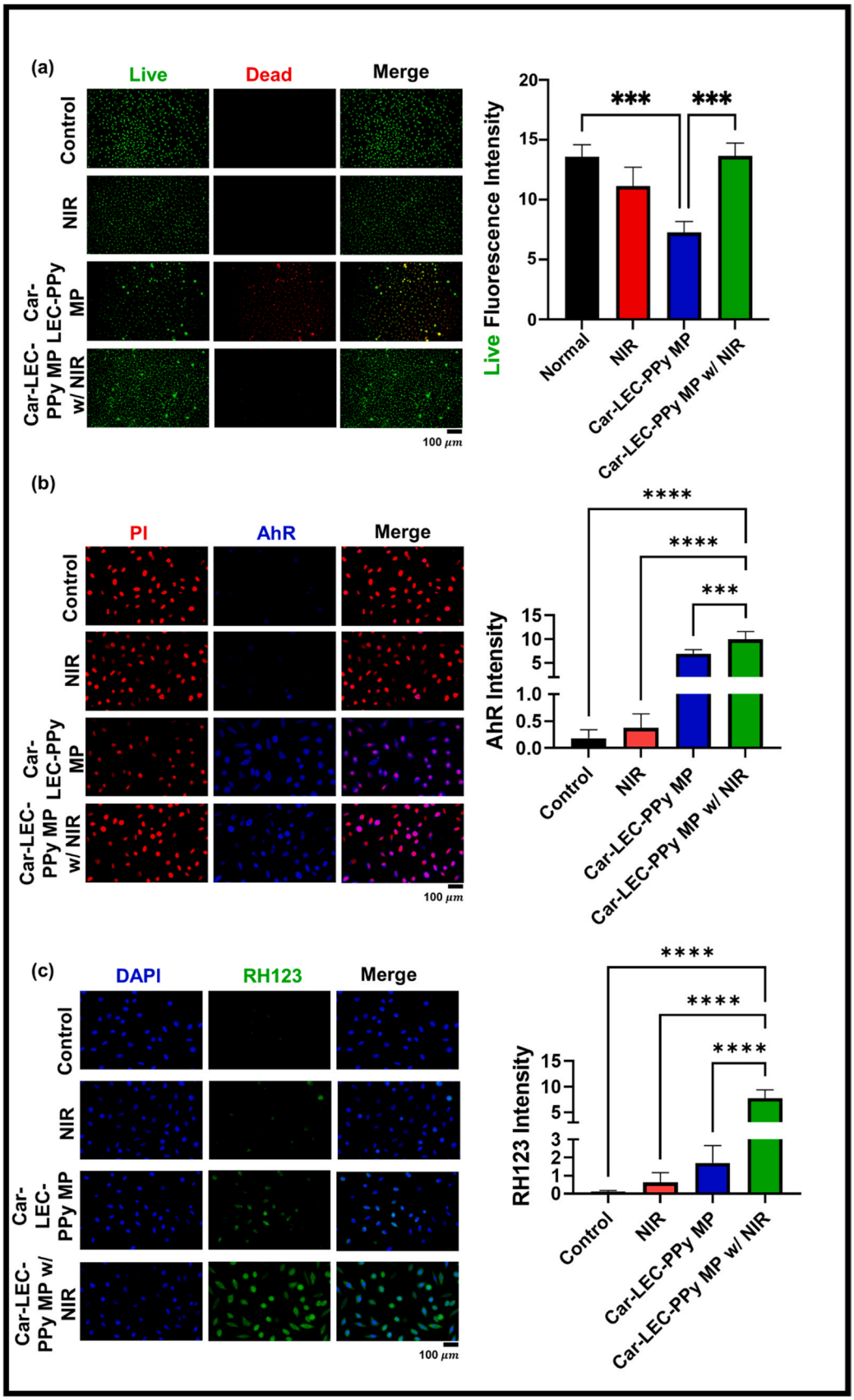

Fig. 2. Analysis of cellular mitochondrial activation, AhR, and RH123 Expression in L929 Cells Treated with Car-LEC-PPy Microparticles. (a) Live/Dead Assay Results. (b) Aryl Hydrocarbon Receptor (AhR) Expression Analysis. (c) Rhodamine 123 (RH123) Expression for Mitochondrial Activity Assessment. The scale bar is 100 μm.

commonly used to assess mitochondrial function in live cells [41]. The mitochondrial membrane potential (ΔΨm) is integral to cellular energy storage and the production of ATP via ATP synthase. After 14 days, blood analysis showed comparable hematological parameters between the Car-LEC-PPy MPs group and the normal group. RBC counts were 9.27 M/μL and 7.26 M/μL, reticulocyte levels were 293.9 K/μL and 287 K/μL, and WBC counts were 5.85 K/μL and 7.4 K/μL, respectively. Platelet counts were stable across groups, and schistocyte levels remained low and similar, indicating minimal hemolysis (Figure S6).

3.3. *In vivo assessments of Car-LEC-PPy MP*

The results of the animal experiments (Fig. 3a) demonstrate that the Car-LEC-PPy MP aqueous solution can be successfully injected into the leg muscles of ICR mice via a syringe. Following near-infrared (NIR) irradiation, as depicted by the temperature changes, the localized temperature within the tissue rose to levels consistent with mild hyperthermia. Histopathological analysis (Fig. 3b) using H&E staining indicated that there was no significant tissue damage in any of the experimental groups Normal, NIR only, Car-LEC-PPy MP only, and Car-LEC-PPy MP + NIR only in the heart, liver, spleen, lung, kidney, and muscle tissues. These results suggest that the phototherapeutic Car-LEC-PPy MP formulation exhibits excellent biocompatibility and does not induce observable histological toxicity, confirming its biosafety for in vivo applications. The histological TUNEL data (Fig. S5) indicated that the Car-LEC-PPy MP formulation combined with NIR might alleviate concerns regarding apoptotic effects.

Further analysis of the fluorescence staining from tissue sections (Fig. 4) revealed the biological effects of the treatment on the different experimental groups. Specifically, the group receiving the Car-LEC-PPy MP injection combined with NIR irradiation (leg + Car-LEC-PPy MP + NIR) showed markedly higher expression of biomarkers, such as Aryl

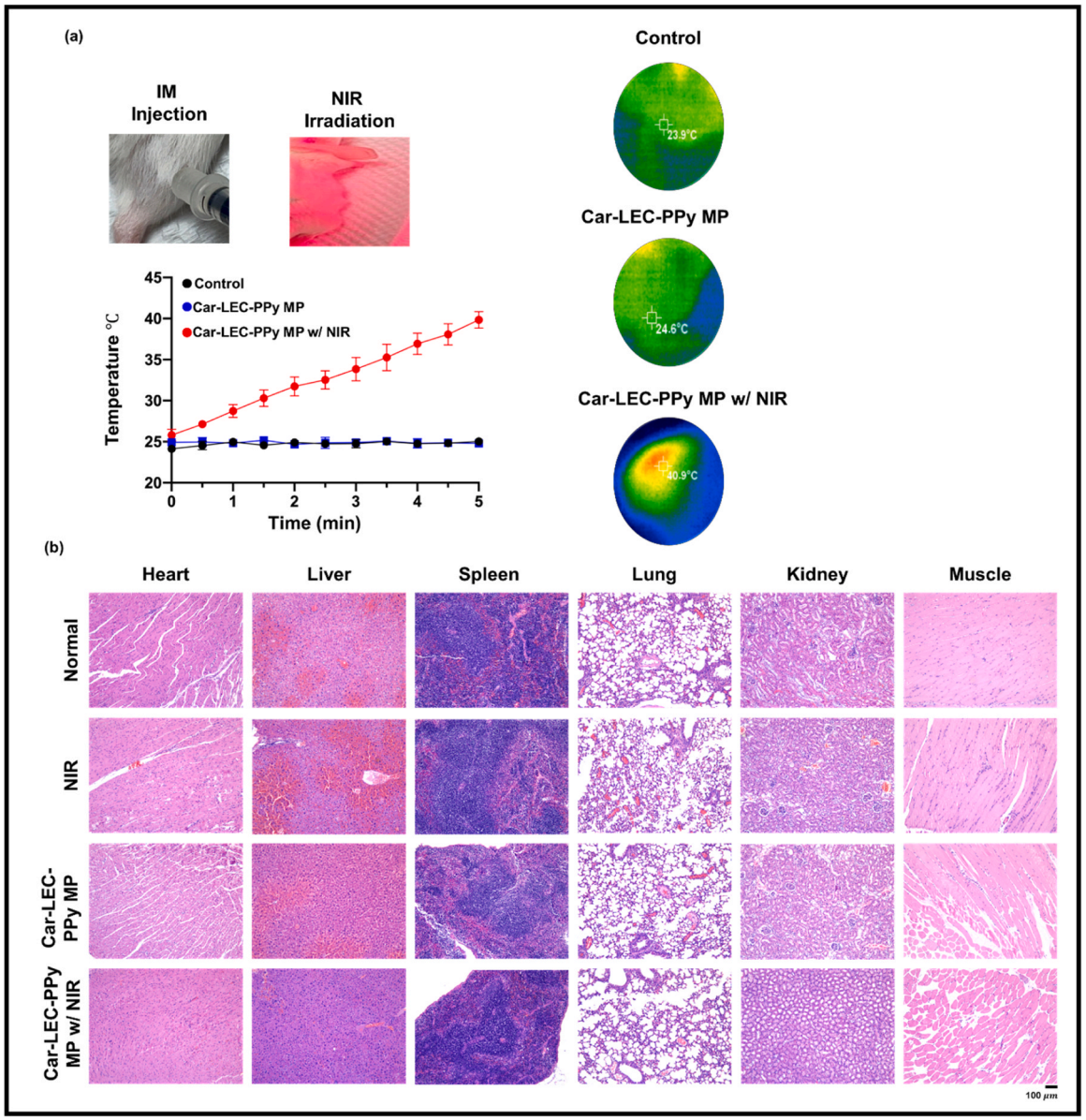

Fig. 3. (a) Injection of Car-LEC-PPy MP aqueous solution into the leg muscles of ICR mice using a syringe. The procedure demonstrates successful delivery of the formulation into muscle tissue. Temperature changes following near-infrared (NIR) irradiation, showing an increase in localized tissue temperature to mild hyperthermia levels. (b) Histopathological analysis via H&E staining of various tissues (heart, liver, spleen, lung, kidney, and muscle) from different experimental groups—control, leg + NIR, leg + Car-LEC-PPy MP, and leg + Car-LEC-PPy MP + NIR—showed no significant tissue damage, demonstrating the biosafety and biocompatibility of the Car-LEC-PPy MP formulation. The scale bar is 100 μm.

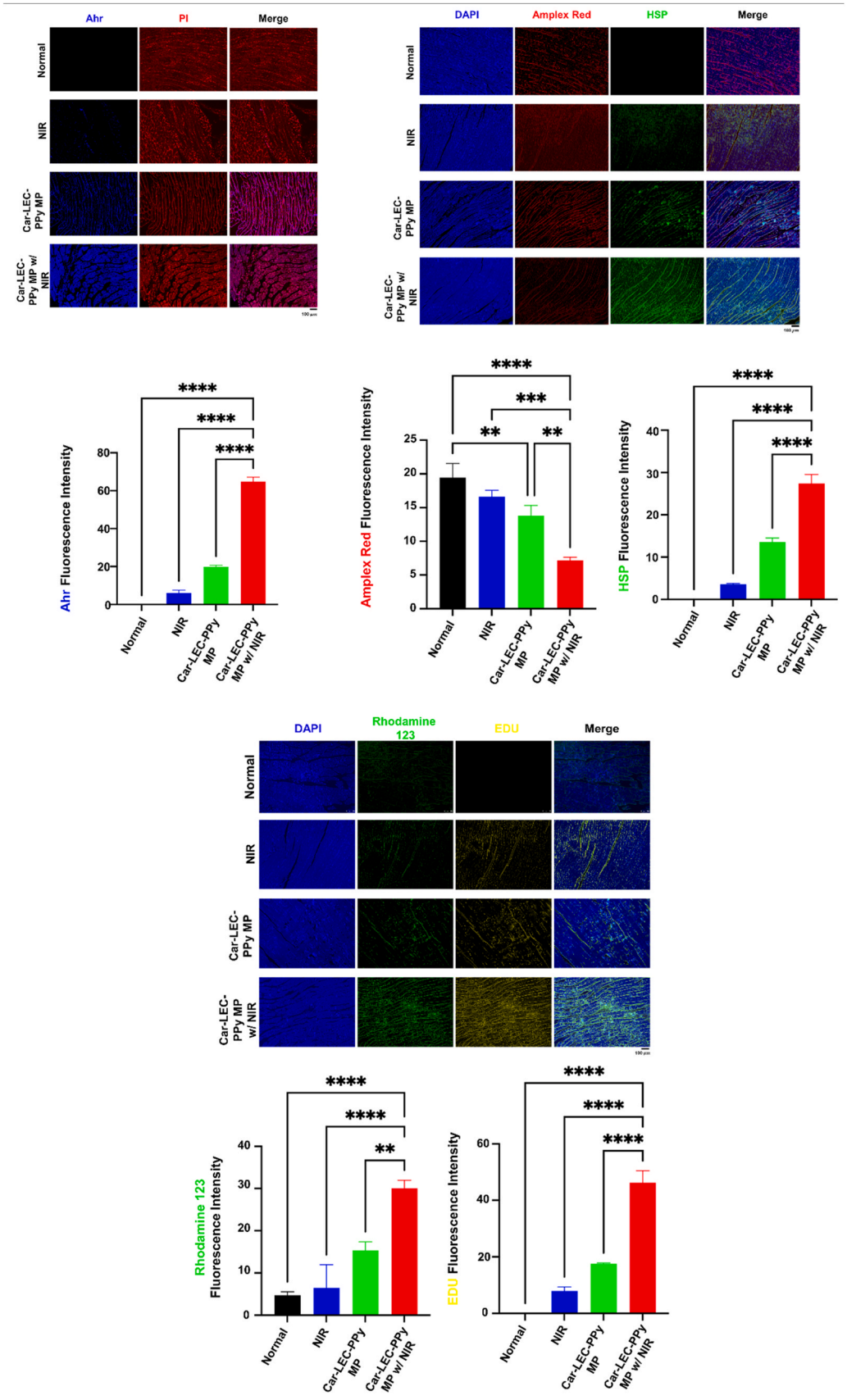

(caption on next page)

Fig. 4. Fluorescence staining analysis of tissue sections from different experimental groups—control, leg + NIR, leg + Car-LEC-PPy MP, and leg + Car-LEC-PPy MP + NIR—revealing biological effects on the tissues. The group treated with Car-LEC-PPy MP + NIR exhibited higher expression levels of Aryl hydrocarbon Receptor (AhR) and Heat Shock Proteins (HSP), increased mitochondrial membrane potential as indicated by Rhodamine 123, and enhanced cellular activity as shown by elevated 5-Ethynyl-2′-deoxyuridine (EDU) incorporation. Additionally, this group demonstrated reduced oxidative stress, highlighting the therapeutic potential of the Car-LEC-PPy MP + NIR combination for promoting mitochondrial activation and cellular resilience. The scale bar is 100 μm.

hydrocarbon Receptor (AhR) and Heat Shock Proteins (HSP), and low ROS, compared to the control group, leg + NIR, and leg + Car-LEC-PPy MP groups. Additionally, this group exhibited elevated levels of Rhodamine 123, indicating enhanced mitochondrial membrane potential, and higher 5-Ethynyl-2′-deoxyuridine (EDU) incorporation, suggesting increased cellular proliferation and activity. Importantly, oxidative stress levels were lower in the Car-LEC-PPy MP + NIR group compared to the others.

4. Conclusion

Our study highlights the importance of understanding the biochemical pathways potentially involved in the activation process of Car-LEC-PPy microparticles. Future research endeavors should focus on elucidating these pathways further to optimize the formulation for clinical applications. This optimization process will ensure that the innovative approach of intercellular mitochondrial activation can be effectively translated into therapeutic strategies. By continuing to explore and refine the mechanisms underlying the therapeutic effects of Car-LEC-PPy microparticles, we can harness their full potential to address unmet medical needs and improve patient outcomes in regenerative medicine and beyond.

CRediT authorship contribution statement

Sih-Chi Chuang: Investigation. **Shih-An Yu:** Investigation. **Pei-Wei Weng:** Investigation. **Hieu Trung Nguyen:** Writing – review & editing, Conceptualization. **Andrew E.-Y. Chuang:** Investigation. **Hieu Trung Nguyen:** Investigation. **Yao-Tung Tsai:** Investigation. **Lekshmi Rethi:** Investigation. **Hsu-Wei Fang:** Investigation. **Pei-Chia Hung:** Investigation. **Jia-Wei Liang:** Writing – review & editing, Methodology, Investigation, Data curation.

Consent for publication

All of the authors involved in this study have agreed to the publication of this manuscript.

Declaration of Competing Interest

The authors declare that they have no known competing financial interests or personal relationships that could have appeared to influence the work reported in this paper.

Acknowledgments

This study was financially supported by grants from the National Science and Technology Council (NSTC), Taiwan [grant numbers 112-2221-E-038-002 -MY3, and 112-2622-E-038–006-].

Appendix A. Supporting information

Supplementary data associated with this article can be found in the online version at doi:10.1016/j.colsurfb.2025.114787.

Data availability

Data will be made available on request.

References

[1] S. Wu, H. Wang, Y. Wei, L. Kang, T. Cui, Y. Huang, Z. Liu, F. Pu, J. Ren, Mitochondria-mediated self-cycling nanoreactor enabling uninterrupted oxidative damage for enhanced chemodynamic therapy, Colloids Surf. B Biointerfaces 240 (2024) 113990.
[2] Y. Huang, G. Liu, F. Zheng, J. Chen, Y. Lin, J. Wang, Y. Huang, Y. Peng, Asymmetric silicon phthalocyanine based nanoparticle with spatiotemporally targeting of mitochondria for synergistic apoptosis-ferroptosis antitumor treatment, Colloids Surf. B Biointerfaces 238 (2024) 113890.
[3] H.L. Zhang, Y. Wang, Q. Tang, C.B. Wang, M.J. Chen, S.P. Yang, J.G. Liu, A mitochondria-targeted multifunctional nanoplatform combining carbon monoxide delivery with O(2)-independent free radical burst under 1064 nm light irradiation for efficient hypoxic tumor therapy, Colloids Surf. B Biointerfaces 230 (2023) 113513.
[4] S. Yang, S. Wang, Y. Zhang, Y. Wang, J. Yuan, Y. Jiang, X. He, L. Liu, J. Song, L. Chen, H. Yang, Heterojunction structured BiOCl-Bi(2)S(3) nanosheets as mitochondria-targeted near-infrared photothermal and photodynamic therapy agent, Colloids Surf. B Biointerfaces 222 (2023) 113106.
[5] X. Gong, Z. Wang, L. Zhang, W. Dong, R. Wang, Y. Liu, S. Song, Q. Hu, F. Du, S. Shuang, C. Dong, A novel carbon-nanodots-based theranostic nano-drug delivery system for mitochondria-targeted imaging and glutathione-activated delivering camptothecin, Colloids Surf. B Biointerfaces 218 (2022) 112712.
[6] R.J. Youle, A.M.V.D. Bliek, Mitochondrial fission, fusion, and stress, Science (New York, N.Y.) 337 (2012) 1062–1065.
[7] J.A. Nicolás-Ávila, A.V. Lechuga-Vieco, L. Esteban-Martínez, M. Sánchez-Díaz, E. Díaz-García, D.J. Santiago, A. Rubio-Ponce, J.L. Li, A. Balachander, J. A. Quintana, A network of macrophages supports mitochondrial homeostasis in the heart, Cell 183 (2020) 94–109, e123.
[8] M.N. Islam, S.R. Das, M.T. Emin, M. Wei, L. Sun, K. Westphalen, D.J. Rowlands, S. K. Quadri, S. Bhattacharya, J. Bhattacharya, Mitochondrial transfer from bone-marrow–derived stromal cells to pulmonary alveoli protects against acute lung injury,, Nat. Med. 18 (2012) 759–765.
[9] K. Hayakawa, E. Esposito, X. Wang, Y. Terasaki, Y. Liu, C. Xing, X. Ji, E.H. Lo, Transfer of mitochondria from astrocytes to neurons after stroke, Nature 535 (2016) 551–555.
[10] E.F. Fang, Y. Hou, K. Palikaras, B.A. Adriaanse, J.S. Kerr, B. Yang, S. Lautrup, M. M. Hasan-Olive, D. Caponio, X. Dan, Mitophagy inhibits amyloid-β and tau pathology and reverses cognitive deficits in models of Alzheimer's disease, Nat. Neurosci. 22 (2019) 401–412.
[11] T. Liao, L. Xiong, X. Wang, S. Yang, Z. Liang, Mitochondrial disorders as a mechanism for the development of obese Sarcopenia, Diabetol. Metab. Syndr. 15 (2023) 224.
[12] A. Caicedo, P.M. Aponte, F. Cabrera, C. Hidalgo, M. Khoury, Artificial mitochondria transfer: current challenges, advances, and future applications, Stem Cells Int. 2017 (2017) 7610414.
[13] M. Picard, T. Taivassalo, D. Ritchie, K.J. Wright, M.M. Thomas, C. Romestaing, R. T. Hepple, Mitochondrial structure and function are disrupted by standard isolation methods, PloS One 6 (2011) e18317.
[14] J.L. Gollihue, A.G. Rabchevsky, Prospects for therapeutic mitochondrial transplantation, Mitochondrion 35 (2017) 70–79.
[15] D. Jiang, F.-X. Chen, H. Zhou, Y.-Y. Lu, H. Tan, S.-J. Yu, J. Yuan, H. Liu, W. Meng, Z.-B. Jin, Bioenergetic crosstalk between mesenchymal stem cells and various ocular cells through the intercellular trafficking of mitochondria, Theranostics 10 (2020) 7260.
[16] T. Ahmad, S. Mukherjee, B. Pattnaik, M. Kumar, S. Singh, M. Kumar, R. Rehman, B. K. Tiwari, K.A. Jha, A.P. Barhanpurkar, M.R. Wani, S.S. Roy, U. Mabalirajan, B. Ghosh, a. Agrawal, Miro1 regulates intercellular mitochondrial transport & enhances mesenchymal stem cell rescue efficacy, EMBO J. 33 (2014) 994–1010.
[17] V.A. Babenko, D.N. Silachev, V.A. Popkov, L.D. Zorova, I.B. Pevzner, E. Y. Plotnikov, G.T. Sukhikh, D.B.J.M. Zorov, Miro1 enhances mitochondria transfer from multipotent mesenchymal stem cells (MMSC) to neural cells and improves the efficacy of cell recovery, Molecules 23 (2018) 687.
[18] H. Li, C. Wang, T. He, T. Zhao, Y.-y. Chen, Y.-l. Shen, X. Zhang, L.-l. Wang, Mitochondrial transfer from bone marrow mesenchymal stem cells to motor neurons in spinal cord injury rats via gap junction, Theranostics 9 (2019) (2017).
[19] H. Zhang, K.J. Menzies, J. Auwerx, The role of mitochondria in stem cell fate and aging, Development 145 (2018) 143420.
[20] R. Tissier, M. Chenoune, S. Pons, R. Zini, L. Darbera, F. Lidouren, B. Ghaleh, A. Berdeaux, D. Morin, Mild hypothermia reduces per-ischemic reactive oxygen species production and preserves mitochondrial respiratory complexes, Resuscitation 84 (2013) 249–255.
[21] S. Chirumbolo, U. Tirelli, M. Franzini, S. Pandolfi, G. Ricevuti, F. Vaiano, L. Valdenassi, Ozone in the adjunct medical treatment. The round personality of a molecule with hormetic properties, Hum. Exp. Toxicol. 42 (2023), 09603271231218926.

[22] S. Zhang, S. Nie, D. Huang, Y. Feng, M. Xie, A novel polysaccharide from Ganoderma atrum exerts antitumor activity by activating mitochondria-mediated apoptotic pathway and boosting the immune system, J. Agric. Food Chem. 62 (2014) 1581–1589.
[23] N. Bolouki, Y.-N. Hsu, Y.-C. Hsiao, P.-R. Jheng, J.-H. Hsieh, H.-L. Chen, B. W. Mansel, Y.-Y. Yeh, Y.-H. Chen, C.-X. Lu, Cold atmospheric plasma physically reinforced substances of platelets-laden photothermal-responsive methylcellulose complex restores burn wounds, Int. J. Biol. Macromol. 192 (2021) 506–515.
[24] M.K. Satapathy, B. Nyambat, C.-W. Chiang, C.-H. Chen, P.-C. Wong, P.-H. Ho, P.-R. Jheng, T. Burnouf, C.-L. Tseng, E.-Y. Chuang, A gelatin hydrogel-containing nano-organic PEI–Ppy with a photothermal responsive effect for tissue engineering applications,, Molecules 23 (2018) 1256.
[25] O.A. Adeleke, L. Fisher, I.N. Moore, G.A. Nardone, A. Sher, A long-acting thermoresponsive injectable formulation of tin protoporphyrin sustains antitubercular efficacy in a murine infection model, ACS Pharm. Transl. Sci. 4 (2021) 276–287.
[26] Y. Tan, K. Ghandi, Kinetics and mechanism of pyrrole chemical polymerization, Synth. Met. 175 (2013) 183–191.
[27] P. Kaewdee, N. Chandet, G. Rujijanagul, C. Randorn, Multicatalytic properties of nanoparticle CaO2 synthesized by a novel, simple and economical method for wastewater treatment, Catal. Commun. 84 (2016) 151–154.
[28] R. Patil, T. Speaker, Carrageenan as an anionic polymer for aqueous microencapsulation, Drug Deliv. 5 (1998) 179–182.
[29] L.F.B. Nogueira, M.A.E. Cruz, C.B. Tovani, H.B. Lopes, M.M. Beloti, P. Ciancaglini, M. Bottini, A.P. Ramos, Curcumin-loaded carrageenan nanoparticles: Fabrication, characterization, and assessment of the effects on osteoblasts mineralization, Colloids Surf. B: Biointerfaces 217 (2022) 112622.
[30] R. Holze, Overoxidation of intrinsically conducting polymers, Polymers 14 (2022) 1584.
[31] F. Jibran, Z. Memon, R. Siddiqui, Z. Aslam, U. Nisar, R. Imad, M. Raza, Eugenol and liposome-based nanocarriers loaded with eugenol protect against anxiolytic disorder via down regulation of neurokinin-1 receptors in mice, Pak. J. Pharm. Sci. 33 (2020) 2275–2284.
[32] M. Wojasiński, D. Ewa, T. Ciach, Lecithin-based wet chemical precipitation of hydroxyapatite nanoparticles, Colloid Polym. Sci. 293 (2015) 1561–1568.
[33] S. Qayyum, A. Jabeen, Z. Aslam, T. Kanwal, M. Raza, S. Faizi, Synthesis and characterization of novel lecithin derived nano-formulation of octyl and dodecyl gallate for targeting B cell associated Non-Hodgkin's lymphoma, J. Clust. Sci. 34 (2022) 1–11.
[34] P. Perumal, C. Selvin, Red algae-derived k-carrageenan-based proton-conducting electrolytes for the wearable electrical devices, J. Solid State Electrochem. 24 (2020) 2249–2260.
[35] F. Li, T. Choong, S. Soltani, A.Luqman Chuah, S.N.A. Md Jamil, N.N. Amerhaider Nuar, Investigation of glyphosate removal from aqueous solutions using Fenton-like system based on calcium peroxide, Processes 10 (2022) 2045.
[36] I. Ibrahim, S. Yunus, A. Hashim, Relative performance of isopropylamine, pyrrole and pyridine as corrosion inhibitors for carbon steels in saline water at mildly elevated temperatures, Int. J. Sci. Eng. Res. 4 (2013) 1–12.
[37] S. Shrikrushna, J. Kulkarni, Influence of dodecylbenzene sulfonic acid doping on structural, morphological, electrical and optical properties on polypyrrole/3C-SiC nanocomposites, J. Nanomed. Nanotechnol. 06 (2015) 1.
[38] V. Tatri, V. Kulkarni, B. Chitragara, S. Raghavendra, Synthesis, characterization and a.c. conductivity of polypyrrole/Y 2 O 3 composites, Bull. Mater. Sci. 29 (2006) 77–83.
[39] P. Christopher Selvin, P. Perumal, S. Selvasekarapandian, S. Monisha, G. Boopathi, M.V.Leena Chandra, Study of proton-conducting polymer electrolyte based on K-carrageenan and NH4SCN for electrochemical devices, Ionics 24 (2018) 3535–3542.
[40] J. Vondráček, K. Pěnčíková, J. Neča, M. Ciganek, A. Grycová, Z. Dvořák, M. Machala, Assessment of the aryl hydrocarbon receptor-mediated activities of polycyclic aromatic hydrocarbons in a human cell-based reporter gene assay, Environ. Pollut. 220 (2017) 307–316.
[41] P.X. Petit, Flow cytometric analysis of rhodamine 123 fluorescence during modulation of the membrane potential in plant mitochondria, Plant Physiol. 98 (1992) 279–286.